IFN-type-I-mediated signaling is regulated by modulation of STAT2 nuclear export

Thomas Frahm, Hansjörg Hauser* and Mario Köster

Department of Gene Regulation and Differentiation, GBF–German Research Centre for Biotechnology, Mascheroder Weg 1, 38124 Braunschweig, Germany

*Author for correspondence (e-mail: hha@gbf.de)

Accepted 5 December 2005
Journal of Cell Science 119, 1092-1104 Published by The Company of Biologists 2006
doi:10.1242/jcs.02822

Summary

Signaling through the IFN type I receptor is mediated by assembly of the ISGF3 complex consisting of STAT1, STAT2 and IRF9. Whereas STAT1 is instrumentalized by many cytokines, STAT2 is specifically used by type I IFNs. Here, we report that the main regulatory mechanism of nuclear accumulation of STAT2 is nuclear export. We determined the kinetics of nucleocytoplasmic shuttling of STAT2 in living cells. In the absence of IFN, a virtually exclusive cytoplasmic localisation of STAT2 can be detected. Nevertheless, STAT2 is permanently and rapidly shuttling between the cytoplasm and the nucleus. The steady-state localization is explained by a very efficient nuclear export. Our studies indicate that at least two pathways (one of which is CRM1-dependent, the other not yet identified) are responsible for clearing the nucleus from STAT2. The constitutive nucleocytoplasmic shuttling of STAT2 does neither depend on the presence of IRF9 or STAT1, nor does it require tyrosine phosphorylation. Upon treatment with IFN type I, nuclear export of STAT2 is completely abolished in cells used within this study, whereas nuclear import is functioning. This explains the observed nuclear accumulation of STAT2. We have identified a region in the C-terminus of STAT2 that is essential for its almost exclusively cytoplasmic localization in the absence of IFN and responsible for CRM1-specific export.

In comparative studies we show that nucleocytoplasmic shuttling of STAT2 is significantly different from that of STAT1. STAT1 is also shuttling in the absence of IFN, but the exchange rate in unstimulated cells is more than ten times lower. We further show that the latent STAT2 protein has stronger intrinsic nuclear-export activity than STAT1. Together, these observations lead to a model for IFN-type-I-induction in which the receptor-mediated heterodimerization overcomes the slow nuclear import of STAT1 and blocks the strong STAT2 export activity that leads to the accumulation of both signal transducers in the nucleus.

Supplementary material available online at
http://jcs.biologists.org/cgi/content/full/119/6/1092/DC1

Key words: Nucleocytoplasmic shuttling, STAT Proteins, Photobleaching, CRM1-independent export, Type-I-interferon-signaling

Introduction

Interferons (IFNs) reprogram gene expression through the activation of signal transducer and activator of transcription (STAT) family members (Stark et al., 1998; Levy and Darnell, 2002). STAT molecules are latent cytoplasmic transcription factors that are primarily regulated by phosphorylation on specific tyrosine residues. Tyrosine phosphorylation induces the dimerization of STAT proteins and their subsequent accumulation in the nucleus. In response to IFN type I (IFN-α/β), heterodimers of STAT1 and STAT2 are formed. These heterodimers rapidly translocate to the nucleus and assemble with the DNA-binding protein IRF9 to form the ISGF3 complex (Fu et al., 1992; Schindler et al., 1992; Veals et al., 1992). IRF9 is a member of the interferon regulatory factor family characterized by a conserved N-terminal DNA-binding domain that binds to interferon-stimulated response elements (ISREs) (Nguyen et al., 1997). The ISRE regulates the transcriptional induction after IFN-type-I-stimulation. After stimulation of cells with type II IFN (IFN-γ) homodimers of STAT1 are formed (Shuai et al., 1992).

STAT proteins execute their function in the nucleus by binding to regulatory DNA elements. Access to the DNA is achieved by movement of the activated proteins from the cytoplasm to the nucleus. The physical link between both compartments is the nuclear pore complex (NPC), which controls the bi-directional transport of macromolecules (Allen et al., 2000; Ryan and Wente, 2000). The NPC creates an aqueous channel that allows the diffusion of smaller molecules and macromolecules of up to 50 kDa in size. Larger macromolecules have to be transported actively through these channels. Specific signals for import and export are encoded in protein sequences (Mattaj and Englmeier, 1998; Talcott and Moore, 1999). Receptors that recognize the nuclear localization signals (NLSs) and the nuclear export signals (NESs) as well as associated molecules for the nucleocytoplasmic transport pathways have been identified. These importins and exportins constitute a family of shuttling transport factors (Weis, 1998). One of the exportins, chromosome region maintenance 1 (CRM1), together with the GTPase Ran recognizes short, leucine-rich, hydrophobic

peptide motifs (Fornerod et al., 1997). The use of leptomycin B (LMB) or ratjadones, specific inhibitors of CRM1 (Fornerod et al., 1997; Fukuda et al., 1997; Ossareh-Nazari et al., 1997; Wolff et al., 1997; Köster et al., 2003), highlights that steady-state localization of various proteins is a consequence of dynamic exchange rather than strict compartmentalization. The polyketide inhibitors bind specifically to CRM1 and thereby inhibit the formation of complexes consisting of CRM1, RanGTP and NES-containing proteins (Kudo et al., 1998; Kudo et al., 1999). In this way they block nuclear export of all proteins by CRM1.

The nuclear import of activated STAT1 and STAT2 is mediated by their association with at least one particular importin-α family member, importin-α5, followed by importin-β-mediated transfer through the NPC (Sekimoto et al., 1997; Fagerlund et al., 2002; McBride et al., 2002). For their rapid import, activated STATs use a dimer-specific NLS within the DNA-binding domain of both molecules (Fagerlund et al., 2002; McBride et al., 2002). Nuclear turnover of STAT1 is mediated by dephosphorylation, and the subsequent nuclear export by binding of a leucine-rich NES to CRM1 (Haspel et al., 1996; Begitt et al., 2000; McBride et al., 2000). Meyer et al. (Meyer et al., 2003) found that DNA-binding, especially interaction with nonspecific DNA, controls dephosphorylation and thereby nuclear accumulation of STAT1.

In contrast to all other STATs, STAT2 seems to play a special role in signal transduction. Although – under certain conditions – STAT2 is capable to form homodimers, it has no affinity to a consensus STAT-DNA-binding element. Specific DNA recognition takes place after association with the IRF9 protein (Bluyssen and Levy, 1997). Furthermore, in untreated cells STAT2 is localized to the cytoplasm. Other STAT proteins are predominantly found in the cytoplasm but also direct a part of the STAT population to the nucleus.

Since the movement between the cytoplasm and the nucleus is an important control mechanism for the activity of signal transducers, we examined the mechanism(s) of STAT2 transport. To analyze changes in dynamic parameters we used enhanced green fluorescent protein (EGFP)-fusion proteins and photobleaching techniques. The strict absence of STAT2 from the nucleus of unstimulated cells was of particular interest. We found that STAT2 is permanently shuttling in this state. A powerful nuclear export process that makes use of two different mechanisms, is responsible for the observed cytoplasmic localization. One of these mechanism acts through the CRM1 nuclear-export receptor, whereas the other pathway is unknown. Interestingly, we found that IFN-β treatment of the cells blocks the nuclear export of STAT2 while import is ongoing.

Results

Permanent nucleocytoplasmic shuttling of endogenous STAT2 in the absence of IFNs

The effect of LMB on IFN-β signaling was analyzed in human fibrosarcoma (2fTGH) cells. Subcellular localization of endogenous STAT2 during stimulation with IFN-β in the absence or presence of LMB was visualized by immunofluorescence staining and analyzed by confocal microscopy. Fig. 1A shows that, in the non-activated state STAT2 localized primarily in the cytoplasm. Stimulation of the cells with IFN-β induced a rapid nuclear accumulation of STAT2. Cytoplasmic relocalization was detectable 4 hours after onset of stimulation and was completed after 8 hours. In the presence of LMB, IFN-β-dependent nuclear translocation of STAT2 was not affected but relocalization to the cytoplasm during the first 4 hours of induction was blocked (Fig. 1A, lower panel). Even 8 hours after stimulation, predominantly nuclear STAT2 was detected in 20-30% of all cells, whereas the remaining cells showed a random distribution of cellular STAT2.

Although LMB is known to inhibit nuclear export, extended nuclear accumulation of STAT2 in the presence of LMB might be due to an indirect effect that leads to reduced dephosphorylation. To rule this out, the time course of STAT2 tyrosine phosphorylation after stimulation with IFN-β was determined by western blotting. As shown in Fig. 1B, IFN-β-induced tyrosine phosphorylation of STAT2 was at its maximum after 1 hour of treatment and decreased slightly within the next hour. After 4 hours of stimulation, only a little remainder of tyrosine-phosphorylated STAT2 was detectable. The decrease parallels the relocation to the cytoplasm as seen in Fig. 1A. Importantly, cells treated with IFN-β and LMB together showed exactly the same kinetics of STAT2 phosphorylation and dephosphorylation as cells treated with IFN-β alone. Further, LMB alone did not induce STAT2 tyrosine phosphorylation, even after 4 hours of treatment (Fig. 1B). Thus, these data suggest that in the first hours following IFN-β stimulation, a CRM1-dependent nuclear export mechanism is predominantly responsible for the cytoplasmic relocalization of STAT2.

To determine whether STAT2 can enter the nucleus in the absence of IFN, the CRM1-dependent export was inhibited by LMB and the subcellular localization of endogenous STAT2 was visualized by confocal analysis after immunostaining. The confocal microscopy and the line-scan analysis shown in Fig. 1C indicate that, LMB induces nuclear accumulation of STAT2, however, only part of the protein population was seen in the nucleus after 2 hours of treatment. Ongoing LMB treatment did not significantly increase the amount of STAT2 in the nucleus further (Fig. 1C). Line-scan analysis was used to demonstrate this in a more quantitative manner. The method also detailed the absence of nuclear STAT2 in untreated cells (Fig. 1C,a). These data indicate that STAT2 is permanently shuttling between the cytoplasm and the nucleus in the absence of IFN. The cytoplasmic steady-state localization of STAT2 is due to an efficient nuclear export. However, the CRM1-dependent mechanism cannot be solely responsible for this efficient nuclear export, suggesting that another, as yet unknown, mechanism must be active in the noninduced state.

IFN-induced transcription by STAT2 requires IRF9 (Kimura et al., 1996). To define the contribution of this factor for the nucleocytoplasmic shuttling of latent STAT2, the mutant cell line U2A, which is defective in IRF9 expression, was used (John et al., 1991). The subcellular localization of endogenous STAT2 was examined in the absence or presence of LMB by immunofluorescence staining (Fig. 1D). In untreated cells, STAT2 localized in the cytoplasm whereas treatment with LMB resulted in nuclear accumulation of the protein. The amount of nuclear STAT2 did not increase when the incubation time was extended. Line-scan analysis demonstrates that in U2A cells, some of the endogenous STAT2 is nuclear – just

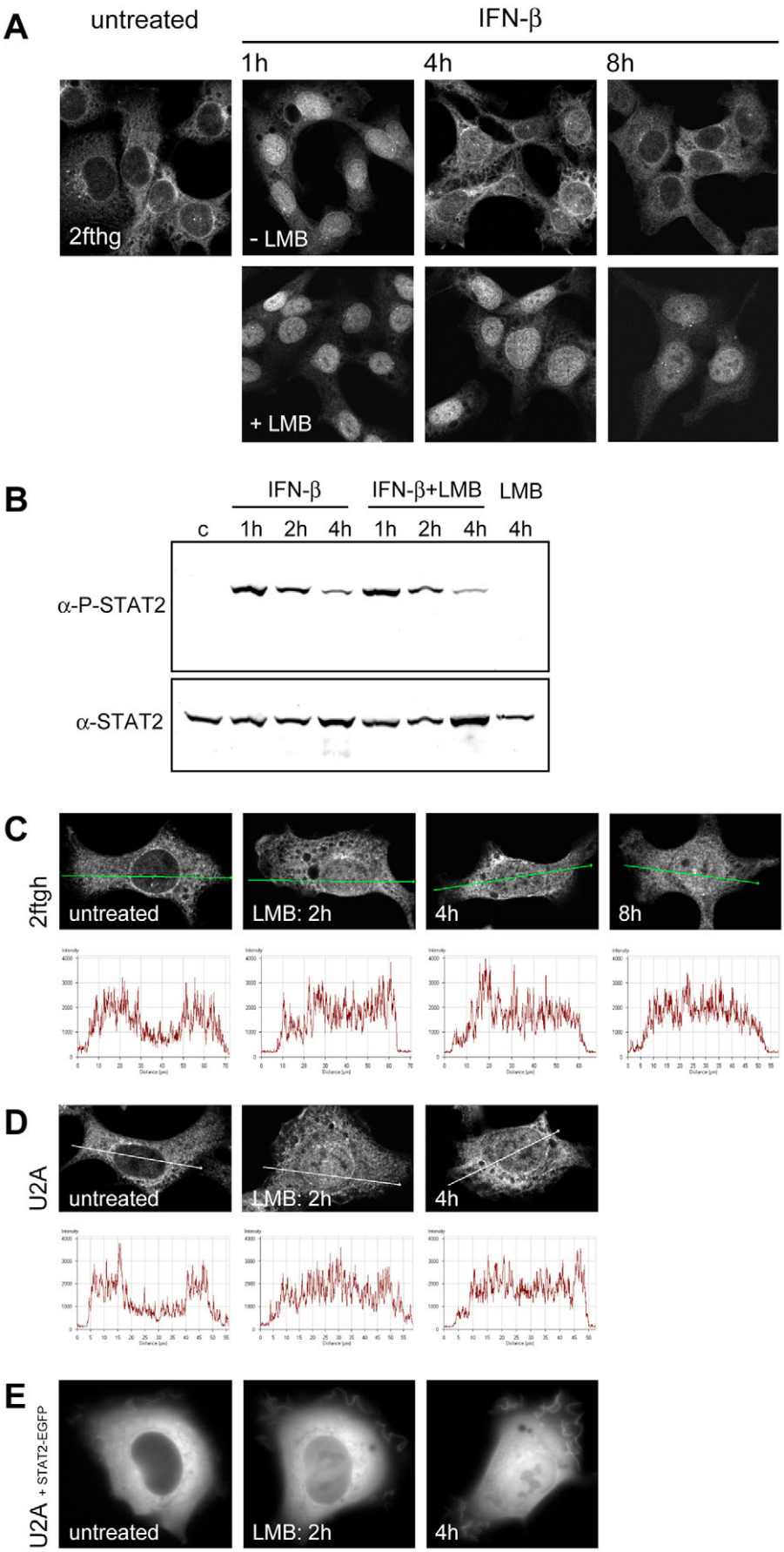

Fig. 1. Effect of CRM1 inhibition on STAT2 nucleocytoplasmic distribution in untreated and IFN-β-stimulated 2fTGH cells. (A) 2fTGH cells were either not treated or were treated with IFN-β for the indicated time periods in the absence (upper panel) or presence of LMB (10 ng/ml) (lower panel). The cells were fixed and stained for STAT2 by indirect immunofluorescence. Fluorescence micrographs were obtained by confocal laser-scanning microscopy. (B) 2fTGH cells were treated as described in A. In addition, LMB alone was added to the cells for 4 hours. Whole-cell extracts were resolved by SDS-PAGE and activated STAT2 was detected with a phosphospecific STAT2-Tyr689 antibody (top). Loading of equal amounts of STAT2 was confirmed by reprobing with STAT2 antiserum (bottom). (C) 2fTGH cells were either left untreated or were treated with LMB (10 ng/ml) for the indicated time periods. Cells were stained for STAT2 and indirect immunofluorescence was analyzed by confocal laser-scanning microscopy. Staining profiles (line-scan analysis) of STAT2 are shown in the lower panel. (D) U2A cells were either left untreated or treated with LMB (10 ng/ml) for the indicated time periods. Cells were stained for STAT2 and analyzed by confocal laser-scanning microscopy. Staining profiles of STAT2 are shown in the lower panel. (E) U2A cells were transiently transfected with STAT2-EGFP expression plasmid. Fourty hours after transfection, subcellular localization of STAT2-EGFP was determined by fluorescence microscopy before and after 2 and 4 hours of LMB treatment.

like in the IRF9-expressing mother cell-line 2fTGH. We, therefore, conclude that IRF9 does not contribute to the constitutive nucleocytoplasmic shuttling of STAT2.

Kinetics of CRM1-independent nuclear export of STAT2-EGFP

Despite nucleocytoplasmic shuttling of STAT2, its nuclear accumulation is prevented by a more efficient nuclear export in the absence of IFN. To study the dynamics of this trafficking process in living cells, we used fluorescence-bleaching techniques and EGFP-fusion proteins, in which the C-terminus of STAT2 was linked to EGFP. The properties of STAT2-EGFP were evaluated following IFN-β stimulation, to ensure that it is fully functional. The fusion protein was expressed in U6A cells, which are deficient in their response to type I IFNs because they lack endogenous STAT2 (Leung et al., 1995). Localization of STAT2-EGFP was determined by fluorescence microscopy before and after treatment with IFN-β. In untreated cells STAT2-EGFP localized in the cytoplasm, whereas efficient accumulation in the nucleus was seen upon stimulation with IFN-β (Fig. 4A). Further evaluation of STAT2-EGFP localization in U6A cells at various time points post-stimulation indicated cytoplasmic relocation with kinetics similar to the endogenous STAT2 in 2fTGH cells. Furthermore, the STAT2-EGFP fusion protein activated an ISRE-driven reporter gene upon IFN-β stimulation of transfected U6A cells to an extent similar to wild-type STAT2 (data not shown). Thus, STAT2-EGFP acts like a functioning STAT2 molecule in IFN-type-I-mediated signal transduction. As reported earlier, a STAT1-GFP fusion protein fulfilled the same features (Köster and Hauser, 1999).

To study the dynamics of STAT-shuttling in individual living cells, alterations in the localization of the fusion proteins STAT1-EGFP and STAT2-EGFP, were analyzed in NIH3T3 cells following treatment with LMB. We found the subcellular distribution of STAT1-EGFP unaltered (Fig. 2A, lower panel); the balance between nuclear and cytoplasmic STAT1-EGFP did not change significantly upon treatment with LMB. By contrast, the essentially cytoplasmic localization of STAT2-EGFP changed (Fig. 2A, upper panel). Single-cell observations showed a successive nuclear accumulation of STAT2-EGFP during the first 3 to 4 hours of treatment. Extended presence of LMB for more than 12 hours, slightly increased the amount of nuclear STAT2-EGFP but did not lead to an exclusive nuclear localization. The same kinetics and the same extent of LMB-induced nuclear accumulation of STAT2-EGFP can be seen in cell lines defective in expression of IRF9 (U2A cells; Fig. 1E) or STAT1 (U3A cells; data not shown), indicating that neither factor is essential for constitutive STAT2-shuttling. Furthermore, we show that the LMB-induced nuclear accumulation of STAT2 does not require its phosphorylation (see supplementary material, Fig. S1).

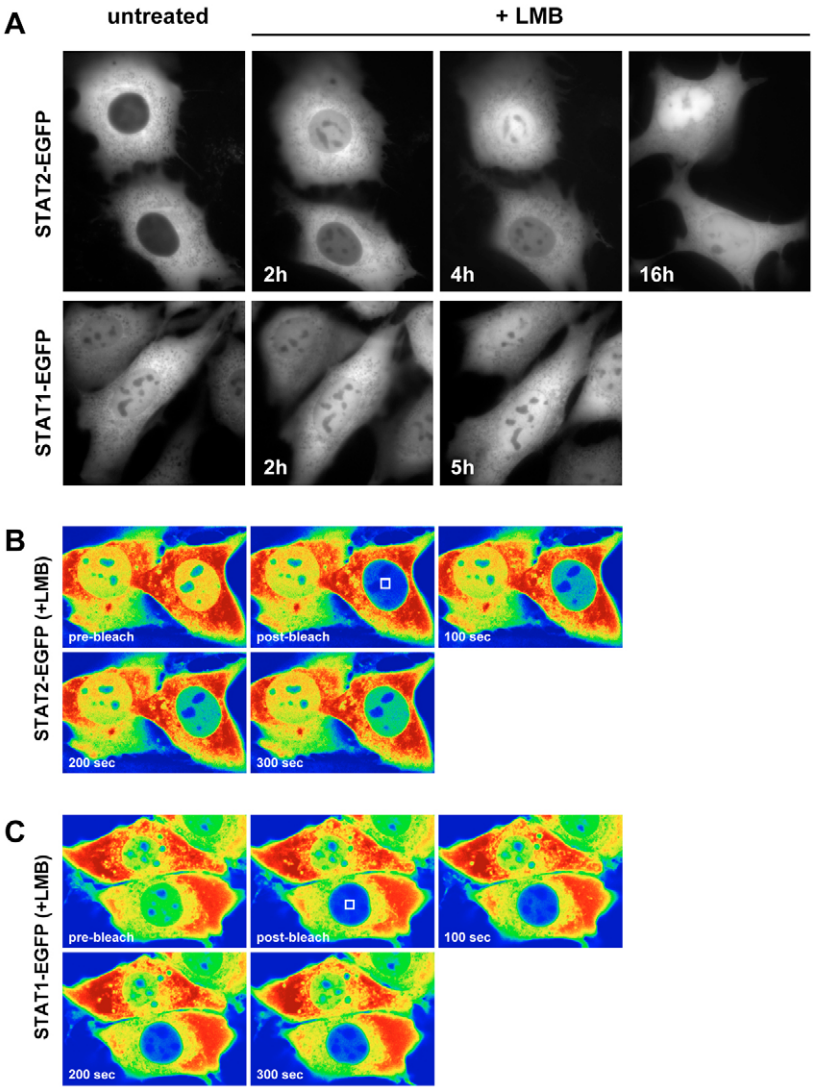

Fig. 2. Kinetics of nuclear import of STAT2-EGFP. (A) LMB induces nuclear accumulation of STAT2-EGFP. NIH3T3 cells stably expressing STAT2-EGFP (top) or STAT1-EGFP (bottom) were treated with LMB (10 ng/ml). Subcellular distribution of STAT2-EGFP and STAT1-EGFP was examined before and at the indicated time points after LMB treatment by fluorescence microscopy. (B) NIH3T3 cells expressing STAT2-EGFP were treated for 2 hours with LMB (10 ng/ml) and subjected to selective FRAP. The indicated area in the nucleus was bleached for 40 seconds. Subsequently, recovery of unbleached STAT2-EGFP into the nucleus was monitored at low-power every 100 seconds. Fluorescence intensity is shown in false color code (intensity increases from blue to red). (C) NIH3T3 were treated as described in B; cells expressing STAT1-EGFP were subjected to selective FRAP.

The kinetics of STAT2-EGFP nuclear translocation (as seen after LMB treatment) was determined by selective fluorescence-recovery after photobleaching (FRAP). NIH3T3 cells stably expressing STAT2-EGFP were treated with LMB for 2 hours. The nucleus was photobleached until the fluorescence in this compartment had entirely disappeared (Fig. 2B). Subsequently, fluorescence-recovery due to movement of unbleached STAT2-EGFP from the cytoplasm

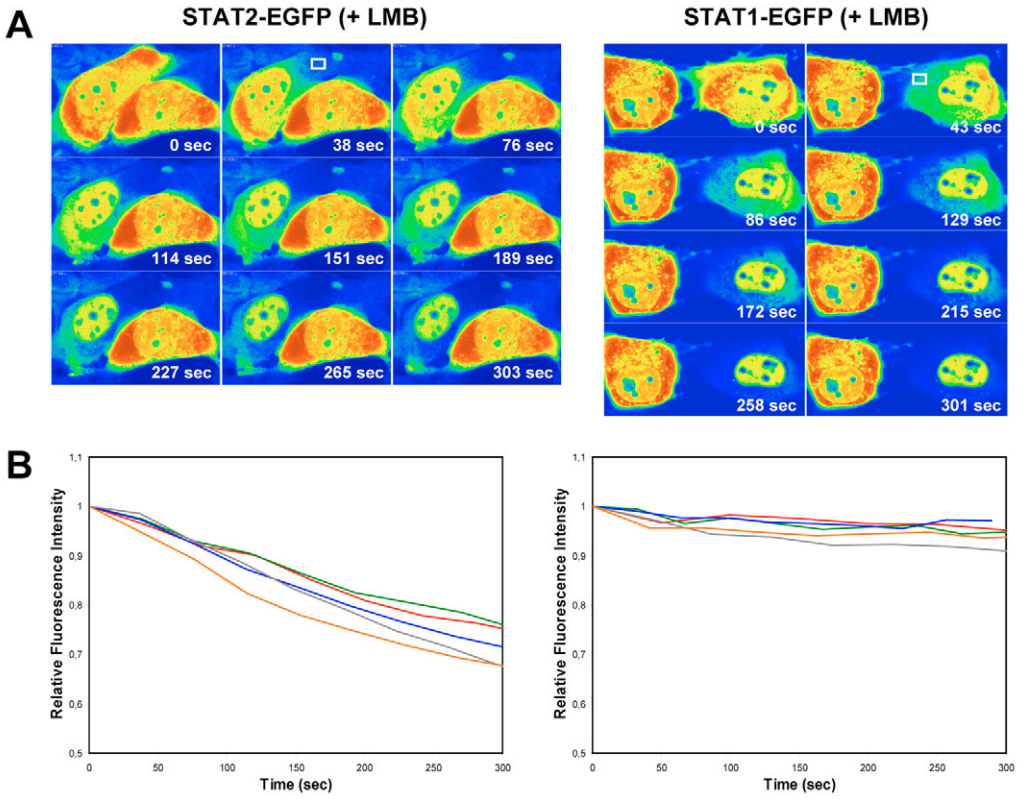

Fig. 3. CRM1-independent nucleocytoplasmic shuttling of STAT2-EGFP. (A) NIH3T3 cells stably expressing STAT2-EGFP (left) or STAT1-EGFP (right) were treated for 4 hours with LMB (10 ng/ml) and subsequently subjected to cytoplasmic FLIP analysis. A cytoplasmic area was bleached with maximum laser intensity by scanning up to nine consecutive periods of 35-43 seconds. The bleached regions are indicated with white rectangles in the first post-bleach images. The total fluorescence of the bleached cells and that of the neighboring cells was monitored between bleaching. The representative image series shows the fluorescence intensities in false color codes (intensity increases from blue to red) before (0 sec) and after the indicated bleaching periods. (B) The nuclear fluorescence intensities of the bleached cells were measured in different experiments, normalized to the total fluorescence of the respective unbleached cells and plotted over time. The relative fluorescence intensities of STAT2-EGFP (left) and STAT1-EGFP (right) in the nucleus are shown during a period of 300 seconds. Colors of graphs reflect individual experiments.

into the nucleus was recorded by sequential imaging scans. Rapid relocation of STAT2-EGFP into the nucleus was seen. Within 5 minutes of post-bleaching, up to 30% of the initial fluorescence-intensity was recovered, indicating a rapid nuclear influx.

Since treatment of cells with LMB results only in an incomplete nuclear accumulation of STAT2-EGFP, it can leave the nucleus in a CRM1-independent way. This CRM1-independent export of STAT2-EGFP was quantitatively measured by using the fluorescence-loss in photobleaching (FLIP) technique. NIH3T3 cells stably expressing STAT2-EGFP were treated with LMB to block CRM1-dependent export (Fig. 3A, left panel). A defined region within the cytoplasm was subjected to repeated photobleaching to prevent recovery of fluorescence in that region. It was therefore possible, to monitor the rate at which fluorescence is lost within the entire cell. Repeated bleaching in a small cytoplasmic region resulted in the complete loss of detectable EGFP-fluorescence in the whole cytoplasm (Fig. 3A). The movement of STAT2-EGFP molecules from distant sites of the cytoplasm caused a certain delay until cytoplasmic fluorescence was completely bleached. The population of fluorescent protein within the nucleus decreased continuously, however, at reduced kinetics. Eventually, the nucleus was also devoid of fluorescence, indicating that all STAT2-EGFP molecules are mobile and can enter the bleached region. The time course of nuclear loss of fluorescence was plotted for several experiments (Fig. 3B, left panel). The data indicate that, within 5 minutes approximately 25% of the nuclear STAT2-EGFP was exported by the CRM1-independent mechanism. This leads to the conclusion that a complete exchange of the STAT2-EGFP molecules between the nuclear and cytoplasmic compartment takes place in less than 20 minutes.

The nucleocytoplasmic shuttling of STAT1-EGFP was compared with that of STAT2-EGFP. NIH3T3 cells stably expressing STAT1-EGFP were established. After a complete nuclear bleaching of STAT1-EGFP in untreated NIH3T3 cells, only very slow recovery of fluorescence in the nucleus was detectable within 5 minutes (Fig. 2C). STAT1-EGFP, therefore, does not shuttle rapidly. This information was supported by results from FLIP experiments. STAT1-EGFP-expressing cells were treated with LMB (Fig. 3A, right panel). The relative loss of fluorescence-intensity of STAT1-EGFP in the nucleus during cytoplasmic bleaching was measured and plotted (Fig. 3B, right panel). Very little of the nuclear STAT1-EGFP had left the nucleus within 5 minutes. Thus, during this time period,

no significant exchange of STAT1-EGFP molecules between the nucleus and cytoplasm was taking place. Similar observations were made in experiments without LMB (data not shown). These findings indicate that, the overall nuclear export of latent STAT1-EGFP is slow when compared to the rapid exchange of STAT2-EGFP.

IFN-β blocks the nuclear export of STAT2

Although in the absence of IFN steady-state pictures localize the STAT2 protein exclusively to the cytoplasm, we have demonstrated that STAT2-EGFP shuttles rapidly between the cytoplasm and the nucleus. However, treatment with IFN-β results in an accumulation of STAT2 in the nucleus. This picture could be caused by stimulation of nuclear-import efficiency or by inhibition of the STAT2 nuclear-export activities. The first hypothesis is based on an ongoing shuttling process, however, with an altered equilibrium that leads to a steady-state equilibrium of nuclear STAT2. To determine which model applies to the nuclear accumulation of STAT2, we treated STAT2-EGFP-expressing U6A cells with IFN-β and performed FLIP experiments. After an initial lack-phase of 10-15 minutes, increasing amounts of the fusion protein appeared in the nucleus. At different time frames of IFN stimulation, cells that showed high amounts of nuclear STAT2-EGFP, were subjected to cytoplasmic FLIP analysis. Repeated bleaching of cytoplasmic areas completely abolished any remaining STAT2-EGFP fluorescence throughout the cytoplasm. Therefore, a refill of fluorescent molecules into the nucleus by newly activated STAT2-EGFP can be neglected. However, the nuclear EGFP fluorescence did not decrease during observation time and this result did not change even at extended periods of IFN-β stimulation (Fig. 4A). This indicates that the nuclear export activity of STAT2-EGFP is completely blocked during IFN-β-induced activation. This rapid switch in the export rate leads to nuclear accumulation of STAT2, indicating that the nuclear-export activity rather than a strong increase in the nuclear-import rate is the main control mechanism that regulates the presence of activated STAT2 in the nucleus.

Next, we asked whether IFN-β treatment specifically blocks the export of STAT2 or induces a general reduction in the nuclear export activity. To answer this question, we used a p50-EGFP-reporter protein, which additionally contains a heterologous NES derived from the HIV Rev protein (Fisher et al., 1995). It was shown that nuclear export mediated by the Rev-NES depends on CRM1 activity (Fornerod et al., 1997). The addition of this NES converts the p50-EGFP to a protein that shuttles permanently between the cytoplasm and the nucleus. The fluorescent population within the nucleus decreased continuously during repeated cytoplasmic bleaching of untreated cells (Fig. 4B). IFN-β stimulation of 2fTGH cells did not alter the nucleocytoplasmic shuttling whereas LMB addition completely blocked nuclear export activity. This finding further indicates that LMB concentrations used here, completely block the export activity of CRM1. We therefore

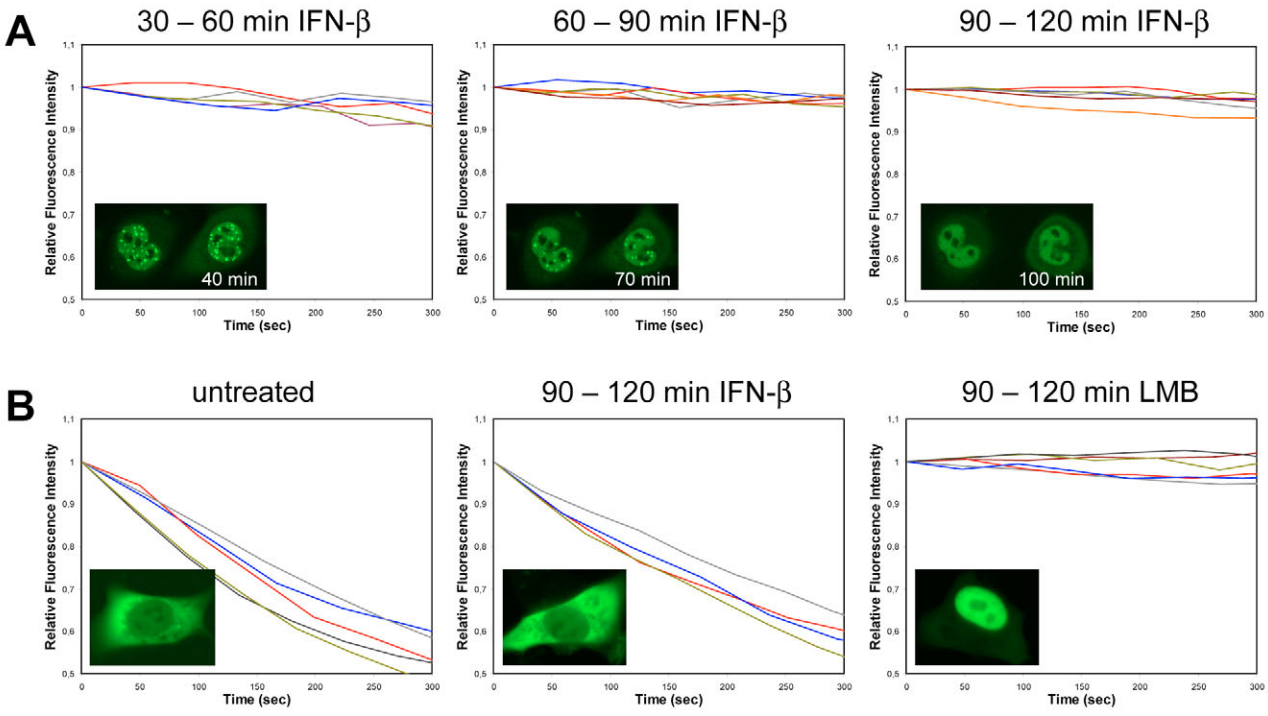

Fig. 4. Stimulation of IFN-β blocks nuclear export of STAT2-EGFP. (A) U6A cells stably expressing STAT2-EGFP were treated with IFN-β. At different times after treatment cytoplasmic FLIP analysis was performed using the same settings as described in Fig. 3. The fluorescence intensities of STAT2-EGFP in the nucleus of the bleached cells were measured, normalized to the total fluorescence of the unbleached cells and plotted over time. Relative fluorescence intensities at the indicated time periods after IFN-β stimulation are shown. The localization of STAT2-EGFP during IFN-β stimulation was documented by showing representative cells for the indicated time points. (B) 2fTGH cells expressing p50-GNES were subjected to cytoplasmic FLIP analysis. Relative nuclear fluorescence intensities are shown for untreated, IFN-β-stimulated and LMB-treated cells. Insets show confocal images of representative cells. Colors of graphs reflect individual experiments.

conclude that IFN-β stimulation specifically affects the nuclear export of STAT2.

The constitutive nuclear export of STAT2 is much stronger than of STAT1

The steady-state of nucleocytoplasmic protein distribution is defined by the speed of nuclear import and export. To compare the nuclear export capacity of both STAT molecules, we normalized their import efficiency by adding a strong NLS. The NLS of the SV40 large T-antigen was added to the C-terminus of the EGFP moiety to create the fusion proteins STAT1-GNLS and STAT2-GNLS, respectively. Their subcellular localization was examined and we found that the balance between nuclear and cytoplasmic localization is indeed altered (Fig. 5A). In the absence of IFN, STAT1-GNLS exclusively localized in the nucleus whereas STAT2-GNLS was still predominantly cytoplasmic with some of the protein in the nucleus. To confirm that the extra NLS was equally active in STAT2-GNLS, we blocked its CRM1-dependent nuclear export by LMB. LMB treatment induced a rapid and complete nuclear accumulation of STAT2-GNLS (Fig. 5A). Thus, by adding an extra NLS to STAT2 the balance of nuclear import and export was shifted only slightly, suggesting that STAT2 owns stronger constitutive export signals compared with those of STAT1.

The STAT2-GNLS fusion protein allowed us to determine the nuclear export rate without addition of LMB, by using the cytoplasmic FLIP approach. The fluorescence of STAT2-GNLS in the nucleus was measured in several experiments and the relative nuclear fluorescence intensity was plotted as a function of time (Fig. 5B; closed lines). Repeated bleaching in the cytoplasm lead to a continuous loss of fluorescent STAT2-GNLS molecules in the nucleus. Compared to the situation of LMB-induced nuclear accumulation of STAT2-EGFP, the decrease of nuclear fluorescence intensity of STAT2-GNLS was higher. This supports the hypothesis of two independent export mechanisms. The same type of experiment carried out with STAT1-GNLS confirmed the slow export capacity of STAT1 (Fig. 5B, dotted lines).

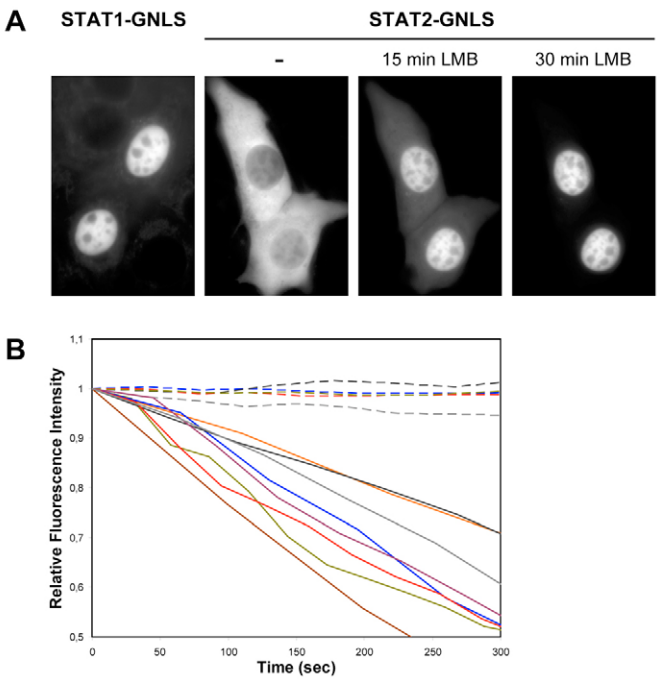

Fig. 5. STAT2 contains a strong constitutive nuclear export signal. (A) C243 cells were transfected with either STAT1-GNLS or STAT2-GNLS as indicated. Localization of the fluorescent proteins was determined in untreated cells by fluorescence microscopy. The effect of LMB was monitored in the same cells on STAT2-GNLS 15 and 30 minutes after treatment. (B) C243 cells transfected with STAT2-GNLS or STAT1-GNLS were subjected to cytoplasmic FLIP analysis using the same settings as described in Fig. 3A. The nuclear fluorescence intensities of the bleached cells were determined in different experiments, normalized to the total fluorescence of the unbleached cells and plotted over time. The relative nuclear fluorescence intensities of STAT2-GNLS (solid lines) and STAT1-GNLS (broken lines) are shown during a time period of 300 seconds. Colors of graphs reflect individual experiments.

Identification of an NES within the C-terminus of STAT2

The interaction between CRM1 and its export substrate requires the presence of an NES within the cargo substrate. NES elements are composed of hydrophobic amino acid (aa) stretches, particularly leucine and/or isoleucine residues (Wen et al., 1995; Kim et al., 1996). The human STAT2 contains several leucine-rich sequences in the C-terminal region that fit characterized NES elements. We assessed the ability of this region for its contribution to nuclear export. Mutants, whose C-terminus was truncated at aa position 754 or 703 were fused to enhanced yellow fluorescent protein (EYFP) and tested for subcellular localization. For this series of mutants, EYFP instead of EGFP was used to allow colocalization analysis with CFP-tagged STAT1. STAT2-Δ754-EYFP, like the full-length protein, localized exclusively to the cytoplasm (Fig. 6B,a), whereas the mutant lacking the C-terminus beyond position 703 localized also to the nucleus (Fig. 6B,b). Several stretches of leucine residues fitting a consensus NES are located between aa 754 and 703 (Fig. 6A). We introduced single leucine-to-alanine mutations at position 733 or 747, as well as a double mutation at position 737/741 into full-length STAT2 and monitored the subcellular distribution of the corresponding EYFP fusion proteins. STAT2 mutants containing L733A or L747A substitutions exhibited a cytoplasmic localization in unstimulated cells (Fig. 6B,c,d). By contrast, substitution of both leucine residues at positions 737 and 741 resulted in an equal distribution (Fig. 6B,e). The mutant showed the same nucleocytoplasmic distribution as the wild-type STAT2 fusion protein after treatment of C243 cells with LMB. Localization of STAT2-LL737/741AA-EYFP was examined in the presence of LMB. Interestingly, LMB did not further increase its nuclear accumulation (Fig. 6B,f). This suggests that this region mediates the CRM1-dependent nuclear export function of STAT2.

Tyrosine phosphorylation of the double mutant was checked in untreated cells and found to be negative (data not shown). Interestingly, IRF9 was not necessary for the constitutive nuclear presence of STAT2-LL737/741AA-EYFP, because transfection of this mutant into U2A cells revealed the same quantity of nuclear fluorescence as IRF9-expressing cell lines NIH3T3 and C243 (Fig. 6B,g).

To investigate the function of the L737A-L741A mutation, the nuclear turnover of STAT2 during and after IFN-β

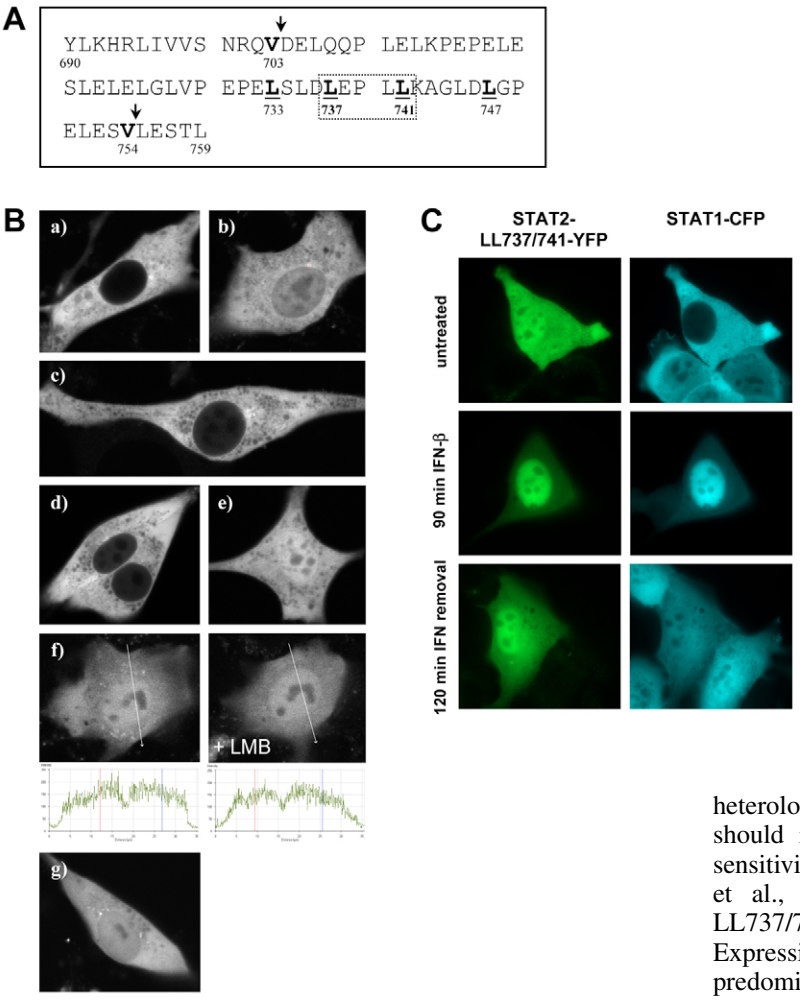

Fig. 6. Characterization of a CRM1 specific STAT2 NES element. (A) Sequence of human STAT2 between aa position 690 and 759. Positions of STAT2 C-terminal deletion mutants are marked by arrows and aa mutated to alanine are underlined. (B) Subcellular localization of STAT2-Δ754-EYFP (a), STAT2-Δ703-EYFP (b), STAT2-L733A-EGFP (c), STAT2-L747A-EGFP (d) and STAT2-LL737/741AA-EYFP (e) was monitored in untreated C243 cells by confocal analysis after transient transfection. Nucleocytoplasmic distribution (f) of STAT2-LL737/741AA-EYFP was compared in C243 cells (left) before and (right) after LMB treatment for 2 hours. The nuclear region is enclosed by the blue and red lines inside the graph of the staining profile. (g) Localization STAT2-LL737/741AA-EYFP was monitored after its transfection into U2A cells. (C) NIH3T3 cells stably expressing STAT1-CFP were transiently transfected with STAT2-LL737/741AA-EYFP expression plasmid. Subcellular localization of both STATs was determined by fluorescence microscopy in untreated cells and after stimulation with IFN-β for 90 minutes. IFN was removed and nucleocytoplasmic distribution of STAT2-LL737/741AA-EYFP and STAT1-CFP was monitored 120 min later.

stimulation was determined. The STAT2-LL737/741AA-EYFP construct was expressed together with STAT1-CFP. The simultaneous monitoring of STAT1-CFP and STAT2-LL737/741AA-EYFP localization should enable us to exclude differences between individual cells (Fig. 6C). Treatment of cells with IFN-β induced simultaneous nuclear accumulation of STAT1-CFP and STAT2-LL737/741AA-EYFP. At different time points after IFN-β removal, STAT2-LL737/741AA-EYFP started to relocalize to the cytoplasm simultaneously with STAT1-CFP (Fig. 6C and data not shown). Therefore, we conclude that in the shut-off period that follows IFN signalling, the CRM1-independent export pathway contributes to nuclear export of STAT2.

To determine the speed of STAT2-LL737/741AA-EYFP-shuttling in the uninduced state, FLIP analysis was carried out. The fluorescent protein population within the nucleus decreased continuously during repeated cytoplasmic bleaching (Fig. 7A). The relative nuclear fluorescence intensity during the time course of the experiment was plotted for several experiments as a function of time (Fig. 7B). During the observation time an exchange of bleached and unbleached STAT2-LL737/741AA-EYFP molecules between the nuclear compartment and the cytoplasm took place. This suggests that the mutant is shuttling, despite the destruction of the C-terminal NES-like element. If this is correct, the addition of a heterologous NES to the STAT2-LL737/741AA-EYFP mutant should rescue the essentially cytoplasmic localization and sensitivity to LMB. The NES of the HIV Rev protein (Fischer et al., 1995) was fused to the C-terminus of STAT2-LL737/741AA-EYFP to create STAT2-LL737/741AA-YNES. Expression of STAT2-LL737/741AA-YNES resulted in a predominant cytoplasmic localization (Fig. 7C) and treatment with LMB caused its nuclear accumulation until an equal distribution between nucleus and cytoplasm was reached. Extended treatment with LMB did not further increase nuclear accumulation (data not shown). To compare the kinetics of nucleocytoplasmic shuttling of STAT2-LL737/741AA-YNES (in cells treated with LMB) with STAT2-LL737/741AA-EYFP (in untreated cells), cells were subjected to cytoplasmic FLIP analysis. The rate of nucleocytoplasmic exchange was revealed to be identical (Fig. 7D). Therefore, we conclude that mutant STAT2-LL737/741AA-EYFP cannot be exported by the CRM1-dependent mechanism and uses only the CRM1-independent pathway for nuclear export. This suggests that the mutation destroys the CRM1-dependent nuclear export function of STAT2 and leaves the CRM1-independent export activity intact.

Next, we tried to describe the contribution of the CRM1-independent mechanism to the overall export activity. Therefore, the strength of the remaining export activity in the STAT2-LL737/741AA mutant was compared with that of the wild-type protein. The EGFP-NLS protein tag was fused to STAT2-LL737/741AA (resulting in STAT2-LL737/741AA-GNLS). In contrast to STAT2-GNLS, the mutant STAT2-LL737/741AA-GNLS localized predominantly in the nucleus (compare Fig. 7C with Fig. 5A). This indicates that the remaining CRM1-independent export activity of STAT2-LL737/741AA-GNLS cannot compensate for the additional strong import signal. To further monitor CRM1-independent

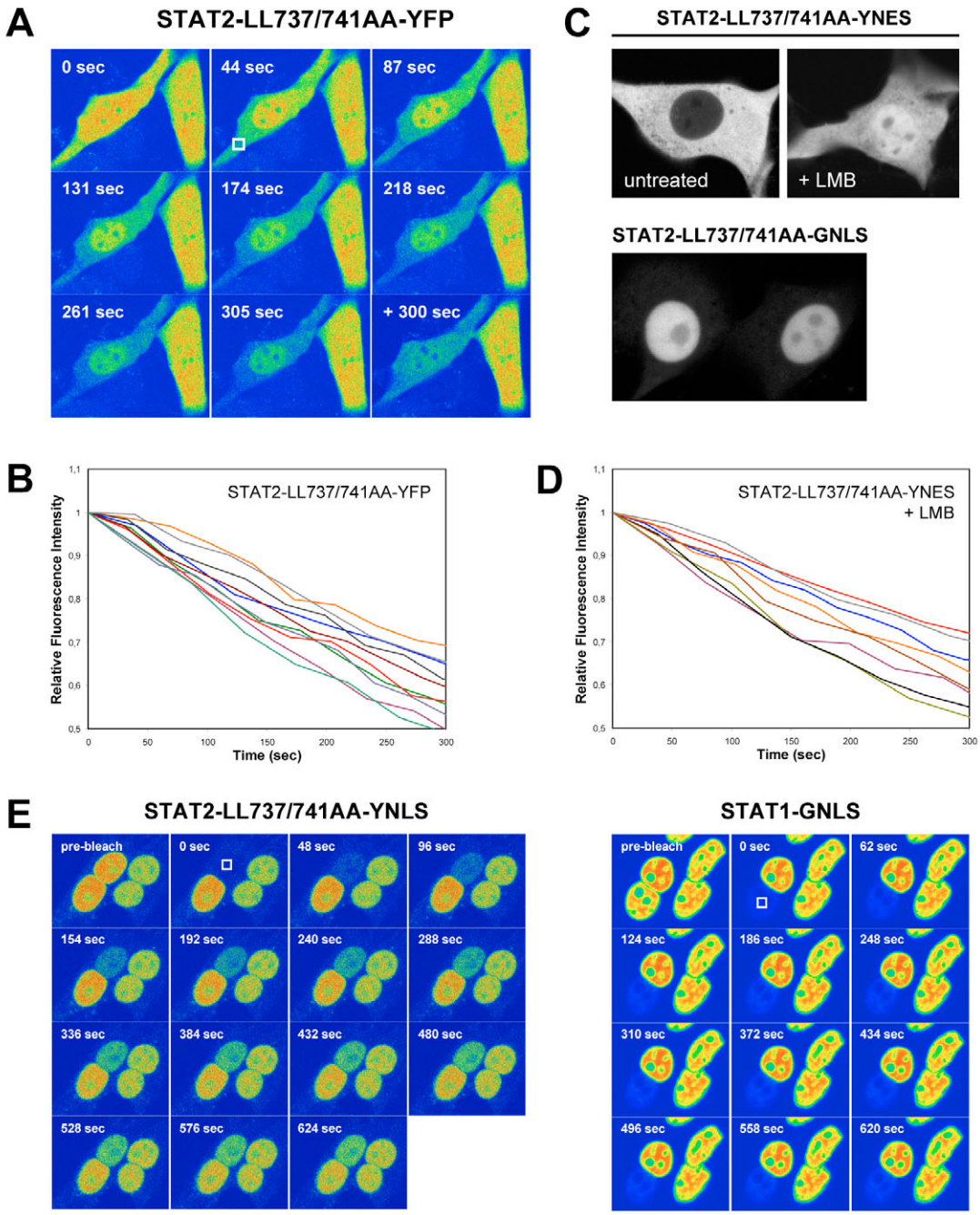

Fig. 7. Characterization of CRM1-independent shuttling of the STAT2 NES mutants STAT2-LL737/741AA. (A) C243 cells were transfected with STAT2-LL737/741AA-EYFP and subjected to cytoplasmic FLIP analysis. The bleach area is indicated with a white square in the first post-bleach image. The representative image series shows the fluorescence intensity in false color code (intensity increases from blue to red) before (0 sec) and after the consecutive bleaching periods. After the last bleach pulse subcellular distribution of STAT2-LL737/741AA-EYFP was monitored after another 300 seconds (+300 sec). (B) The nuclear fluorescence intensities of the bleached cells from A were measured in different experiments, normalized to the total fluorescence of the unbleached cells and plotted over time. Relative fluorescence intensities of STAT2-LL737/741AA-EYFP in the nucleus are shown. Colors of graphs reflect individual experiments. (C) C243 cells were transfected with either STAT2-LL737/741AA-YNES or STAT2-LL737/741AA-GNLS as indicated. Localization was determined in untreated cells by confocal analysis. The effect of LMB was monitored on STAT2-LL737/741AA-YNES localization 1 hour after treatment. (D) C243 cells expressing STAT2-LL737/741AA-YNES were treated for 4 hours with LMB (10 ng/ml) and subsequently subjected to FLIP analysis as described in A. Relative nuclear fluorescence intensities of STAT2-LL737/741AA-YNES from different experiments are shown. (E) C243 cells expressing STAT2-LL737/741AA-GNLS (left) or STAT1-GNLS (right) were pre-treated with cytochalasin D to induce bi-nuclear cells. The indicated area in one nucleus of a single cell was bleached until complete loss of fluorescence. Subsequently, recovery of unbleached STAT2-LL737/741AA-GNLS and STAT1-GNLS molecules into the nucleus was monitored for 10 minutes. Representative image-series show fluorescence intensities in false color code (increasing from blue to red) for the bleached cells (left) and neighboring cells (right) prior to bleaching and after the indicated post-bleach time periods.

nuclear export activity of STAT2-LL737/741AA, we subjected cells expressing STAT2-LL737/741AA-GNLS to a FRAP-based bikaryon assay. Bikaryons were created by treating cells with the actin-microfilament-disrupting toxin cytochalasin D, to generate multi-nucleated cells. Cytochalasin D does not inhibit IFN-α- and IFN-γ-induced signal transduction, indicating that nuclear trafficking of the STATs would not affected (Lillemeier et al., 2001). C243 cells expressing STAT2-LL737/741AA-GNLS were treated with cytochalasin D and binuclear cells were subjected to selective FRAP analysis. One nucleus of a binuclear cell was photobleached until the complete loss of fluorescence was observed. Subsequently, fluorescence recovery due to movement of unbleached molecules from the non-bleached nucleus was recorded by sequential imaging scans. Fig. 7E shows that nuclear recovery of STAT2-LL737/741AA-GNLS was clearly visible 30 seconds after bleaching. Visualization of fluorescence intensities at later time points show an inverse correlation between the increase of fluorescent molecules in the bleached nucleus and the decrease of fluorescence in the unbleached one. The fluorescence in the control cell remained stable. The same experiment was carried out for STAT1-GNLS-expressing cells (Fig. 7F). The results show that recovery of fluorescence in the bleached nucleus is very slow indicating that STAT1 shuttling in the non-activated state is much slower compared with the STAT2 shuttling.

Discussion

To investigate the nucleocytoplasmic shuttling of STAT1 and STAT2 in real time, we used STAT1- and STAT2-EGFP fusion proteins. Relevant aspects of functionality of the fusion proteins were checked. The kinetics of nuclear accumulation and tyrosine phosphorylation of STAT1-EGFP is indistinguishable from that of endogenous STAT1 (Köster and Hauser, 1999) (M.K., unpublished data). Furthermore, dimer formation of STAT1-GFP with the endogenous STAT1 protein occurs after IFN-γ-induced activation of STAT (Lillemeier et al., 2001), and identical transactivation capacities were determined for the wild-type and the fusion protein (Köster and Hauser, 1999). We found that the STAT2-EGFP fusion protein is fully functional in IFN-β-mediated transcriptional activation and that it interacts with STAT1 and IRF9 (this report, and M.K., unpublished data). These controls therefore allow the conclusion that wild-type STAT2 and STAT2-EGFP have similar properties, and that the results achieved with the fusion protein will also apply for the wild-type protein. Photobleaching experiments allowed us to determine the kinetics of nucleocytoplasmic shuttling within a short time-frame. Therefore, small changes in the exchange rate could be quantified.

We analyzed the nucleocytoplasmic shuttling of latent STAT2 in living cells. The results shown here reveal that, before induction with IFN, STAT2 shuttles rapidly between the nucleus and the cytoplasm. In unstimulated cells the ability of STAT2 to enter the nucleus depends neither on tyrosine phosphorylation nor on the presence of STAT1 and IRF9, the other components of the ISGF3 complex. In the absence of IFN, the steady-state localization of STAT2 is predominantly cytoplasmic, and results from a dominant nuclear export activity. During this latent phase, STAT2 uses two nuclear export pathways simultaneously. One depends on CRM1, whereas another mechanism acts independently of CRM1. The kinetics of nuclear import and nuclear export are not influenced by the presence of STAT1 or IRF9, indicating that STAT2 shuttling is independent of both proteins.

All experiments were carried out in mouse and human cell lines with essentially the same results. However, smaller differences with respect to the kinetics of shuttling were found between the cell lines and individual clones thereof. It is noteworthy to say that only human STAT1 and STAT2 were studied in all cell types.

One finding was unexpected. The shuttling rate of STAT2 is so high that a complete cycle of exchange takes less than 20 minutes; the corresponding movement of STAT1 in these cells, however, is more than 10 times slower. This is due to differential nuclear import and export kinetics, although it is well known that, after IFN stimulation, both molecules heterodimerize and then must share at least the kinetics of nuclear import.

The biological meaning of the rapid STAT2 movement is not immediately clear. One question concerns its ability to transactivate. STAT2 as such has no affinity to the consensus STAT-DNA-binding element or the IFN-stimulated response element (ISRE). For ISRE-binding, the IRF9 protein is needed. Martinez-Moczygemba et al. detected a strong constitutive interaction of STAT2 with IRF9 in co-immunoprecipitation experiments (Martinez-Moczygemba et al., 1997). This interaction does not depend on the presence of IFN. Using different techniques, we confirmed these results with STAT2 fusion proteins (M.K., unpublished data). The resulting potential to bind DNA and activate transcription might be important. In case STAT2 would accumulate in the nucleus, IRF9 could recruit it to promoter sites and induce a basal expression of some IFN-stimulated genes (ISGs). However, it seems that a complete clearance of STAT2 in unstimulated cells is most probably related to the total absence of transcription of some of these genes. In this context, we recognized a toxic effect of stably expressed STAT2-GNLS or STAT2-LL737/741AA-EYFP in different cell lines (data not shown). Thus, changing the balance between STAT2 nuclear import and export might cause unknown changes in cellular physiology leading to cell death. This might explain why independent nuclear export mechanisms act together to clear STAT2 from the nucleus in the absence of IFN and after termination of IFN signaling.

A sequence motif was identified within the STAT2 transactivator domain. This motif fits to a classical NES and was mapped to the region between aa 735 and 743. Point mutations or deletion of this region lead to partial nuclear accumulation of the STAT2 mutants. Banninger and Reich found that mutation of the leucine residues 740 and 741 in full-length STAT2 protein leads to a retarded export after treating the cells with IFN-α (Banninger and Reich, 2004). Fusion of a region that includes the complete STAT2 transactivation domain (aa 652-851) to GFP, directs the chimeric molecule to the cytoplasm. However, we found that shorter fragments, such as aa 731-747, show no obvious export activity (data not shown). Our data indicate that the NES consensus sequence is not sufficient to function as an independent NES. Structural components conferred by the larger STAT2 domain are additionally required.

The data presented here reveal that the efficient nuclear

export of STAT2 is executed by two independent pathways, one depends on CRM1, the other does not. Two arguments suggest that the defined NES-homology sequence is the target of CRM1-specific export. First, LMB treatment does not further increase the partial nuclear presence of the STAT2-LL737/741AA-EYFP mutant. Second, the addition of a heterologous NES to this mutant protein restores its almost exclusively cytoplasmic localization.

Having the strong nuclear export activity of latent STAT2 in mind, the mechanism by which nuclear accumulation after induction of type I IFN is achieved has to be reconsidered. We applied cytoplasmic FLIP experiments to find out whether IFN-β-induced nuclear accumulation of STAT2 is due to a complete block of nuclear export or the creation of an equilibrium - in which nuclear import exceeds nuclear export. Photobleaching experiments clearly demonstrated an almost complete loss of STAT2-EGFP export during the accumulation phase; during the observation time of 5 minutes, no substantial nuclear export of activated STAT2-EGFP was found to occur. We compared the import rates of latent STAT2 with the activated STAT2 molecule by selective FRAP experiments. No obvious increase in the STAT2-EGFP-import rate was detected after treatment with LMB in the presence and absence of IFN-β (data not shown). Therefore, the switch from high- to a low-export activity is the major level that controls the nuclear accumulation of STAT2. These results and evidence from the use of the STAT2-LL737/741AA-EYFP mutant (Fig. 6C) indicate that, during accumulation phase the CRM1-dependent and -independent export mechanisms are switched off. Termination of IFN-receptor-mediated signaling goes along with regaining both STAT2 export activities.

Based on these data, a model for the action of IFN type I can be deduced. IFN-induced receptor stimulation initiates phosphorylation and heterodimerization of STAT1 and STAT2. These heterodimers have properties that resemble STAT2 with respect to nuclear import, i.e. STAT1 adapts the speed of STAT2. STAT1 is probably transported as well through the efficient STAT2-specific import mechanism. However, this dimer has lost its export activity and therefore accumulates in the nucleus. Possibly, the nuclear export signals are hidden or inactivated in the dimeric conformation. Dephosphorylation of the dimer in the nucleus allows dissociation of both molecules and leads to the reactivation of their export properties. The model does not explain whether the activation of genes is purely due to the enhanced presence of STAT2 or whether the dimeric conformation is the transcriptional transactivator.

Banninger and Reich reported that the nuclear translocation of latent STAT2 depends on its constitutive association with IRF9 (Banninger and Reich, 2004). By contrast, we found no differences in the nucleocytoplasmic distribution of endogenous STAT2 or STAT2-EGFP fusion protein after treatment with LMB in cells expressing IRF9 (NIH3T3, 2fTGH, U3A) or not expressing IRF9 (U2A). This discrepancy is not immediately clear. However, the techniques we used in this study (confocal analysis and time-lapse experiments) clearly point towards an IRF-9-independent nuclear import of STAT2. This is underpinned by the nuclear presence of the STAT2 NES mutant STAT2-LL737/741AA-EYFP in U2A cells.

For other STATs, constitutive nucleocytoplasmic shuttling has been shown. Pranada et al. determined the dynamics of a STAT3-CFPYFP fusion protein by using a pulse bleaching technique (Pranada et al., 2004). STAT3 was found to constitutively shuttle between the cytoplasm and nucleus in unstimulated cells for which tyrosine phosphorylation is not necessary. Meyer et al. showed that in the uninduced state, STAT1 shuttles between the nucleus and the cytoplasm independently of tyrosine phosphorylation (Meyer et al., 2002). Marg et al. further found that the constitutive export of STAT1 is mediated by the CRM1-dependent nuclear export pathway (Marg et al., 2004).

Other transcription factor families show nucleocytoplasmic shuttling. Several reports have demonstrated continuous shuttling of Smads between the nucleus and the cytoplasm before and during TGF-β signaling (Xu et al., 2002; Inman et al., 2002; Nicolás et al., 2004). Smads use different pathways for their nuclear export. Smad4 nuclear export depends of CRM1, whereas Smad2 and Smad3 are exported from the nucleus by a CRM1-independent mechanism. Xu et al. showed that Smad2 interacts directly with the nucleoporins CAN/Nup214 and Nup153 (Xu et al., 2002). These interactions are required for the constitutive nucleocytoplasmic shuttling of Smad2. Marg et al. demonstrated that STAT1 also binds to CAN/Nup214 and Nup153 and this interaction mediates the nuclear import of the latent molecules (Marg et al., 2004). So far it is not clear whether STAT2 uses the same mechanism to mediate the CRM1-independent nuclear export.

Materials and Methods

Plasmid constructions

Genes encoding fusion proteins were created by standard polymerase chain reaction (PCR) techniques using *Pwo* DNA polymerase (Roche). Site-directed mutagenesis was performed using the Quick Change Site-Mutagenesis kit (Stratagene). All PCR-generated DNA fragments and point mutations were controlled by sequencing in the final expression plasmids. Expression of the various human STAT constructs is controlled by the MT7 promoter (Dirks et al., 1994). pSTAT1-EGFP and pSTAT2-EGFP were constructed by replacing the GFP sequence in pSTAT1-GFP and pSTAT2-GFP (Köster and Hauser, 1999), respectively, by the sequence encoding for the enhanced GFP (EGFP) (Clontech). pSTAT2-EYFP encodes for a fusion protein of STAT2 with the enhanced yellow fluorescent protein (EYFP) (Clontech). In pSTAT1-CFP the EGFP sequence was replaced by the sequence encoding for cyan fluorescent protein (CFP) (Clontech). The C-terminal deletion mutants pSTAT2-Δ703-EYFP and pSTAT2-Δ754-EYFP were generated by subcloning PCR fragments into pSTAT2-EYFP. The plasmids pSTAT2-L733A-EGFP, pSTAT2-L747A-EGFP and pSTAT2-LL737/741AA-EYFP were generated by site-directed mutagenesis. pSTAT1-GNLS, pSTAT2-GNLS and pSTAT2-LL737/741AA-GNLS contain the NLS of SV40 large T antigen (PKKKRKV) C-terminally linked to EGFP. pSTAT2-LL737/741AA-YNES and p50-GNES contain the NES of the HIV Rev protein (LPPLERLTL) at the C-terminus of EYFP and EGFP, respectively.

Cell culture, gene transfer and induction of cells

Murine fibroblast C243 cells, NIH3T3 cells, and the human fibrosarcoma cell lines 2fTGH, U2A and U6A (Pellegrini et al., 1989; John et al., 1991; Leung et al., 1995) were maintained in Dulbecco's modifed Eagle's medium (DMEM) supplemented with 10% fetal calf serum, antibiotics, and glutamine. C243 and NIH3T3 cell lines were transfected by using the calcium phosphate co-precipitation method (Graham and van der Eb, 1973). Transfection of U2A and U6A cell lines was performed with GenePorter2 (Gene Therapy Systems Inc.), according to the manufacturer's instructions. Cells were stimulated with 500 units/ml human or mouse IFN-β. Leptomycin B (kindly provided by M. Yosida, University of Tokyo) was used at a final concentration of 10 ng/ml. To generate multi-nucleated cells, C243 cells were treated with cytochalasin D (Sigma) at a final concentration of 2.5 μg/ml 16 to 20 hours before analysis. Cells were washed with PBS, fresh growth medium was added and FRAP analysis was performed 1 hour later.

Western blotting

Following treatment, whole cell extracts were prepared using ice-cold lysis buffer containing 50 mM Tris-HCl pH 7.5, 150 mM NaCl, 1 mM EDTA, 1% Triton X-100, 0.5% NP40, 1 mM Na_3VO_4, 1 mM NaF, 500 μM 4-(2-aminoethyl)

benzenesulphonyl fluoride (AEBSF), 150 nM aprotinin, 1 μM E-64 and 1 μM leupeptin. Extracts were clarified by centrifugation and separated by SDS-PAGE. Proteins were transferred to nitrocellulose membrane (Amersham Biosciences) and detected by western blotting with anti-(Tyr689)Phospho STAT2 antibody (Upstate Biotechnology) followed by secondary antibody and enhanced chemiluminescence (ECL) detection system (Amersham Biosciences). After phosphotyrosine detection, membranes were stripped and reprobed with STAT2 antibody (C-20, Santa Cruz Biotechnology).

Immunofluorescence microscopy and image acquisition

For indirect immunofluorescence, cells grown on coverslips were fixed for 5 minutes with cold (–20°C) methanol/acetone (1:1) and blocked in PBS containing 3% bovine serum albumin. The cells were incubated for 1 hour with the primary anti-STAT2 antibody (C-20; Santa Cruz Biotechnology). Excess antibody was removed by washing three times with PBS containing 0.1% saponin. To detect the primary antibody, the samples were incubated for 45 minutes at room temperature with a Cy3-labeled anti-rabbit secondary antibody (Dianova). Cells were washed again in PBS containing 0.1% saponin and then mounted onto glass slides. Fluorescence microscopy of Cy3-labeled antigens was done with a Zeiss Axiovert 135TV microscope equipped for epifluorescence with XF137 filter set from Omega Optical. For visualization of ECFP, EGFP and EYFP the following filter sets from Omega Optical were used: XF114, XF100 and XF104. Images were acquired with a Photometrics high-resolution, cooled charge-coupled device camera (PXL 1400) controlled by IPLab Spectrum software (SignalAnalytics).

Confocal analysis and photobleaching

For time-course studies and photobleaching techniques, cells were placed into Lab-Tek chamber slides (Nunc) at least 20 hours before analysis. Confocal analysis was performed with a Zeiss LSM 510 META inverted confocal laser-scanning microscope equipped with an on-stage heating chamber using a Plan-Apochromat 100× oil immersion objective (1.3 numeric aperture). Cells expressing EGFP fusion proteins were excited with an argon laser at 488 nm, and emission was collected using a 505-550 nm bandpass filter. For EYFP visualization an argon laser at 514 nm and a 530-600 nm bandpass filter were used. For selective FRAP experiments, an area in the nucleus was scanned with maximum laser power until an extinction of fluorescence in the complete nuclear compartment was observed. Subsequently, total fluorescence of the bleached cell and of a neighboring cell was recorded with minimal laser power by sequential imaging. In FLIP experiments an area of the cytoplasm was bleached by scanning for up to nine consecutive periods of 35-43 seconds with maximum laser intensity. The total fluorescence of the bleached cell and of a neighboring cell was monitored between the times of bleaching with minimal laser power. The unbleached cells in the same image were used to correct the acquired fluorescence intensities for a generalized bleaching effect. Fluorescence intensities of the nuclear compartment of the bleached cells were measured and the obtained raw data were corrected for (1) the background intensity and (2) fluorescence intensity of the unbleached cells. The presented graphs show a normalized plot of nuclear fluorescence intensity versus time.

We thank M. Yoshida for the generous gift of LMB and I. Kerr for cell lines. We further thank G. Müller-Newen for the helpful and constructive discussion. This work was supported by a grant from HFSPO (RG 166/2000-M).

References

Allen, T. D., Cronshaw, J. M., Bagley, S., Kiseleva, E. and Goldberg, M. W. (2000). The nuclear pore complex: mediators of translocation between nucleus and cytoplasm. *J. Cell Sci.* **113**, 1651-1659.

Banninger, G. and Reich, N. C. (2004). STAT2 nuclear trafficking. *J. Biol. Chem.* **279**, 39199-39206.

Begitt, A., Meyer, T., van Rossum, M. and Vinkemeier, U. (2000). Nucleocytoplasmic translocation of Stat1 is regulated by a leucine-rich export signal in the coiled-coil domain. *Proc. Natl. Acad. Sci. USA* **97**, 10418-10423.

Bluyssen, H. A. and Levy, D. E. (1997). Stat2 is a transcriptional activator that requires sequence-specific contacts provided by Stat1 and p48 for stable interaction with DNA. *J. Biol. Chem.* **272**, 4600-4605.

Dirks, W., Schaper, F. and Hauser, H. (1994). A new hybrid promoter directs transcription at identical start points in mammalian cells and in vitro. *Gene* **149**, 389-390.

Fagerlund, R., Melén, K., Kinnunen, L. and Julkunen, I. (2002). Arginine/lysine-rich nuclear localization signals mediate interactions between dimeric STATs and importin alpha 5. *J. Biol. Chem.* **277**, 30072-30078.

Fischer, U., Huber, J., Boelens, W. C., Mattaj, I. W. and Lührmann, R. (1995). The HIV-1 Rev activation domain is a nuclear export signal that accesses an export pathway used by specific cellular RNAs. *Cell* **82**, 475-483.

Fornerod, M., Ohno, M., Yoshida, M. and Mattaj, I. W. (1997). CRM1 is an export receptor for leucine-rich export signals. *Cell* **90**, 1051-1060.

Fu, X.-Y., Schindler, C., Improta, T., Aebersold, R. and Darnell, J. E., Jr (1992). The proteins of ISGF-3, the interferon α-induced transcriptional activator, define a gene family involved in signal transduction. *Proc. Natl. Acad. Sci. USA* **89**, 7840-7843.

Fukuda, M., Asano, S., Nakamura, T., Adachi, M., Yoshida, M., Yanygrida, M. and Nishida, E. (1997). CRM1 is responsible for intracellular transport mediated by the nuclear export signal. *Nature* **390**, 308-311.

Graham, F. L. and van der Eb, A. J. (1973). A new technique for the assay of infectivity of human adenovirus 5 DNA. *Virology* **52**, 456-467.

Haspel, R. L., Salditt-Georgieff, M. and Darnell, J. E., Jr (1996). The rapid inactivation of nuclear tyrosine phosphorylated Stat1 depends upon a protein tyrosine phosphatase. *EMBO J.* **15**, 6262-6268.

Inman, G. J., Nicolás, F. J. and Hill, C. S. (2002). Nucleocytoplasmic shuttling of Smads **2**, 3, and 4 permits sensing of TGF-β receptor activity. *Mol. Cell* **10**, 283-294.

John, J., McKendry, R., Pellegrini, S., Flavell, D., Kerr, I. M. and Stark, G. R. (1991). Isolation and characterization of a new mutant cell line unresponsive to alpha and beta interferons. *Mol. Cell. Biol.* **11**, 4189-4195.

Kim, F. J., Beeche, A. A., Hunter, J. J., Chin, D. J. and Hope, T. J. (1996). Characterization of the nuclear export signal of human T-cell lymphotropic virus type 1 Rex reveals that nuclear export is mediated by position-variable hydrophobic interactions. *Mol. Cell. Biol.* **16**, 5147-5155.

Kimura, T., Kadokawa, Y., Harada, H., Matsumoto, M., Sato, M., Kashiwazaki, Y., Tarutani, M., Tan, R. S., Takasugi, T., Matsuyama, T. et al. (1996). Essential and non-redundant roles of p48 (ISGF3 gamma) and IRF-1 in both type I and type II interferon responses, as revealed by gene targeting studies. *Genes Cells* **1**, 115-124.

Köster, M. and Hauser, H. (1999). Dynamic redistribution of STAT1 protein in IFN signaling visualized by GFP fusion proteins. *Eur. J. Biochem.* **260**, 137-144.

Köster, M., Lykke-Andersen, S., Elnakady, Y. A., Gerth, K., Washausen, P., Höfle, G., Sasse, F., Kjems, J. and Hauser, H. (2003). Ratjadones inhibit nuclear export by blocking CRM1/exportin 1. *Exp. Cell Res.* **286**, 321-331.

Kudo, N., Wolff, B., Sekimoto, T., Schreiner, E. P., Yoneda, Y., Yanagrida, M., Horinouchi, S. and Yoshida, M. (1998). Leptomycin B inhibition of signal-mediated nuclear export by direct binding to CRM1. *Exp. Cell Res.* **242**, 540-547.

Kudo, N., Matsumori, M., Taoka, H., Fujiwara, D., Schreiner, E. P., Wolff, B., Yoshida, M. and Horinouchi, S. (1999). Leptomycin B inactivates CRM1/exportin 1 by covalent modification at a cysteine residue in the central conserved region. *Proc. Natl. Acad. Sci. USA* **96**, 9112-9117.

Leung, S., Qureshi, S. A., Kerr, I. M., Darnell, J. E., Jr and Stark, G. R. (1995). Role of STAT2 in the alpha interferon signaling pathway. *Mol. Cell. Biol.* **15**, 1312-1317.

Levy, D. E. and Darnell, J. E., Jr (2002). STATs: transcriptional control and biological impact. *Nat. Rev. Mol. Cell. Biol.* **3**, 651-662.

Lillemeier, B. F., Köster, M. and Kerr, I. M. (2001). STAT1 from the cell membrane to the DNA. *EMBO J.* **20**, 2508-2517.

Marg, A., Shan, Y., Meyer, T., Meissner, T., Brandenburg, M. and Vinkemeier, U. (2004). Nucleocytoplasmic shuttling by nucleoporins Nup153 and Nup214 and CRM1-dependent nuclear export control the subcellular distribution of latent Stat1. *J. Cell Biol.* **165**, 823-833.

Martinez-Moczygemba, M., Gutch, M. J., French, D. L. and Reich, N. C. (1997). Distinct STAT structure promotes interaction of STAT2 with the p48 subunit of the interferon-alpha-stimulated transcription factor ISGF3. *J. Biol. Chem.* **272**, 20070-20076.

Mattaj, I. W. and Englmeier, L. (1998). Nucleocytoplasmic transport: the soluble phase. *Annu. Rev. Biochem.* **67**, 265-306.

McBride, K. M., McDonald, C. and Reich, N. C. (2000). Nuclear export signal located within the DNA-binding domain of the STAT1 transcription factor. *EMBO J.* **19**, 6196-6206.

McBride, K. M., Banninger, G., McDonald, C. and Reich, N. C. (2002). Regulated nuclear import of the STAT1 transcription factor by direct binding of importin-alpha. *EMBO J.* **21**, 1754-1763.

Meyer, T., Gavenis, K. and Vinkemeier, U. (2002). Cell type-specific and tyrosine phosphorylation-independent nuclear presence of STAT1 and STAT3. *Exp. Cell Res.* **272**, 45-55.

Meyer, T., Marg, A., Lemke, P., Wiesner, B. and Vinkemeier, U. (2003). DNA binding controls inactivation and nuclear accumulation of the transcription factor Stat1. *Genes Dev.* **17**, 1992-2005.

Nguyen, H., Hiscott, J. and Pitha, P. M. (1997). The growing family of interferon regulatory factors. *Cytokine Growth Factor Rev.* **8**, 293-312.

Nicolás, F. J., de Bosscher, K., Schmierer, B. and Hill, C. S. (2004). Analysis of Smad nucleocytoplasmic shuttling in living cells. *J. Cell Sci.* **117**, 4113-4125.

Ossareh-Nazari, B., Bachelerie, F. and Dargemont, C. (1997). Evidence for a role of CRM1 in signal-mediated nuclear protein export. *Science* **278**, 141-144.

Pellegrini, S., John, J., Shearer, M., Kerr, I. M. and Stark, G. R. (1989). Use of a selectable marker regulated by alpha interferon to obtain mutations in the signaling pathway. *Mol. Cell. Biol.* **9**, 4605-4612.

Pranada, A. L., Metz, S., Herrmann, A., Heinrich, P. C. and Müller-Newen, G. (2004). Real time analysis of STAT3 nucleocytoplasmic shuttling. *J. Biol. Chem.* **279**, 15114-15123.

Ryan, K. J. and Wente, S. R. (2000). The nuclear pore complex: a protein machine bridging the nucleus and cytoplasm. *Curr. Opin. Cell Biol.* **12**, 361-371.

Schindler, C., Fu, X.-Y., Improta, T., Aebersold, R. and Darnell, J. E., Jr (1992). Proteins of transcription factor ISGF-3: One gene encodes the 91- and 84-kDa ISGF-3 proteins that are activated by interferon-α. *Proc. Natl. Acad. Sci. USA* **89**, 7836-7839.

Sekimoto, T., Immoto, N., Nakajima, K., Hirano, T. and Yoneda, Y. (1997). Extracellular signal-dependent nuclear import of Stat1 is mediated by nuclear pore-targeting complex formation with NPI-1, but not Rch1. *EMBO J.* **16**, 7067-7077.

Shuai, K., Schindler, C., Prezioso, V. R. and Darnell, J. E., Jr (1992). Activation of transcription by IFN: Tyrosine phosphorylation of a 91-kD DNA binding protein. *Science* **258**, 1808-1812.

Stark, G. R., Kerr, I. M., Williams, B. R. G., Silverman, R. H. and Schreiber, R. D. (1998). How cells respond to interferons. *Annu. Rev. Biochem.* **67**, 227-264.

Talcott, B. and Moore, M. S. (1999). Getting across the nuclear pore complex. *Trends Cell Biol.* **9**, 312-318.

Veals, S. A., Schindler, C., Leonard, D., Fu, X.-Y., Aebersold, R. and Levy, D. E. (1992). Subunit of an IFN-α-responsive transcription factor is related to IRF and Myb families of DNA-binding proteins. *Mol. Cell. Biol.* **12**, 3315-3324.

Weis, K. (1998). Importins and exportins: how to get in and out of the nucleus. *Trends Biochem. Sci.* **23**, 185-189.

Wen, W., Meinkoth, J. L., Tsien, R. Y. and Taylor, S. S. (1995). Identification of a signal for rapid export of proteins from the nucleus. *Cell* **82**, 463-473.

Wolff, B., Sanglier, J.-J. and Wang, Y. (1997). LMB is an inhibitor of nuclear export: inhibition of nucleo-cytoplasmic translocation of the human immunodeficiency virus type 1 (HIV-1) Rev protein and Rev-dependent mRNA. *Chem. Biol.* **4**, 139-147.

Xu, L., Kang, Y., Çöl, S. and Massagué, J. (2002). Smad2 nucleocytoplasmic shuttling by nucleoporins CAN/Nup214 and Nup153 feeds TGF-β signaling complexes in the cytoplasm and nucleus. *Mol. Cell* **10**, 271-282.